

# Effects of Rain on Microwave Remote Sensing Systems and Ground-Based Radars Use in Durban

Chrispin T. Mulangu and Thomas J.O. Afullo, *Senior Member, SAIEE*

**Abstract—** In this paper the results show that for rainfall intensity below about 10 mm/h for Marshall-Palmer (MP), Joss-Drizzle (JD), Joss-Thunderstorm (JT) and Law-Parson (LP) distributions and below about 4 mm/h for Continental-Showers (CS), Tropical Showers (TS), Continental Thunderstorms (CT) and Tropical Thunderstorm (TT) distributions, the specific rain backscattering follows Rayleigh scattering law where the rain drops are small with respect to the wavelength when the frequency is 19.5 GHz. At rain rate above 10 mm/h for exponential distribution and above 4 mm/h for lognormal distribution, the specific backscattering follows Mie scattering law. When received echo power from rain becomes significant, it contributes to the rise in the noise floor and the radar can lose the target. Also the result shows that Mie backscattering efficiency is highest at raindrop diameter of 4.7mm.

**Index Terms—**Specific Rain Backscattering

## I. INTRODUCTION

Hydrometeors are essentially particles of water within the atmosphere, which take the form of liquid water as in rain, mist and fog or ice as in clouds, hail and snow. Plane electromagnetic waves traveling through air containing precipitation are scattered and absorbed by the particles of ice, snow or water. Water, with its larger dielectric constant scatters electromagnetic wave more strongly than ice, [1, 2 and 3]. In addition, it has a much larger dielectric loss and the attenuation due to thermal dissipation is therefore much greater for water particles than for ice particles [4, 5]. This makes rain degrade the performance of millimeter wave and microwave radars more than ice. Radiowave propagating through a rain zone, will be scattered, depolarized, absorbed and delayed in time. All these effects of rain on the wave propagation are related to the frequency at which the signal is transmitted, and polarization of the wave as well as to the rain rate, which influences the form and size distribution of the raindrop.

In this paper we investigate the impact of rain on sensor systems at microwave frequencies in Durban. As there is no measurement on radar, we have used the rain attenuation measurement for the path profile for the 6.73km terrestrial line-of-sight from the Howard College campus to the Westville campus [6-7], since the hydrometeors act in the

same way for both links. We thus investigate the specific backscattering for that link which could be applied to radar systems in Durban and can be used as an indicator for the degree of possible degradation of performance.

Consider Fig. 1, the total field, at a distance  $r$  from a reference point in the particle, in the direction of a unit vector  $k_s$  consists of the incident field  $E_i(r)$  and the field  $E_s$  scattered by the particle. Within a distance  $r < D^2 / \lambda$  where  $D$  is a typical dimension of the particle such as its diameter, the field  $E_s(r)$  has complicated amplitude and phase variations because of interference between contributions from different parts of the particle. So, the observation point  $r$  is said to be in the near field of the particle. When  $r > D^2 / \lambda$  however, the scattered field  $E_s(r)$  behaves as a spherical wave and is given, according to [4, Page 279], by

$$E_s(r) = f(j_i, k_s) \frac{e^{-jkr}}{r} \quad (1)$$

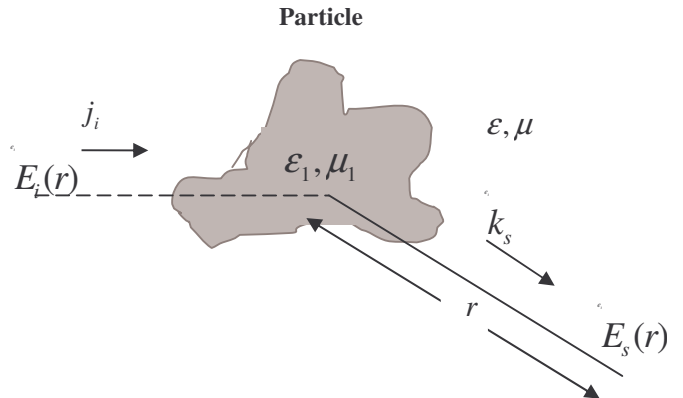


Fig. 1 A plane wave  $E_i(r)$  is incident upon a dielectric scatterer and the scattered field  $E_s(r)$  is observed in the direction  $k_s$  at a distance  $r$ , [4, Page 279].

$f(j_i, k_s)$  represents the amplitude, phase and polarization of the scattered wave in the far field in the direction  $k_s$  when the particle is illuminated by a plane wave propagating in the direction  $j_i$  with unit amplitude. It is known as the scattering amplitude. At frequencies below 6GHz ( $\lambda=5cm$ ), most rain droplet sizes satisfy the condition  $ka \leq 0.1$  and therefore the Rayleigh scattering theory is applicable. Even at 10GHz ( $\lambda=3cm$ ),  $ka$  is much smaller than unity, except for heavy rain, and Rayleigh scattering gives a good approximation. In Rayleigh scattering, the total sum of the

The authors are with the School of Electrical, Electronic & Computer Engineering, University of KwaZulu-Natal, Durban 4041, South Africa. (Corresponding author phone: +27-31-260 2713; fax: +27-31-260 7008; e-mail: afullo@ukzn.ac.za).

cross sections of all particles per unit volume, such as  $\rho < \sigma_s >$ ,  $\rho < \sigma_a >$ ,  $\rho < \sigma_t >$  and  $\rho < \sigma_b >$  we have, [4, pp 46]:

$$\rho < \sigma_s > = \frac{128 \pi^5}{3 \lambda^4} |K|^2 \int_0^\infty a^6 n(a) da \quad (2)$$

$$\rho < \sigma_a > = \frac{8 \pi^2}{\lambda} \text{Im}(K) \int_0^\infty a^3 n(a) da \quad (3)$$

$$\rho < \sigma_t > = \rho < \sigma_s > + \rho < \sigma_a > \quad (4)$$

$$\rho < \sigma_b > = \frac{64 \pi^5}{\lambda^4} |K|^2 \int_0^\infty a^6 n(a) da \quad (5)$$

Where  $t$ ,  $a$ ,  $s$  and  $b$  stand for extinction, absorption, scattering and backscattering and  $K = (\epsilon_r - 1) / (\epsilon_r + 2)$ . The value of  $K$  depends on wavelength and temperature. In the range of  $\lambda = 3$  to  $10 \text{ cm}$ ,  $|K|^2$  is almost constant at temperatures between  $0$  and  $20^\circ \text{C}$  and is equal to  $0.93$ . The imaginary part  $\text{Im}(K)$  ranges from  $0.0074$  at  $20^\circ \text{C}$  to  $0.00688$  at  $10^\circ \text{C}$ . Since rain attenuation is usually small and unimportant at the longer wavelengths where this expression is valid, the simplicity offered by the Rayleigh scattering approximation is of limited use for predicting the attenuation through rain [8]. The computation of the rain attenuation must therefore be based on the exact formulation for spheres as developed by Mie.

The efficiencies  $Q_i$  for the interaction of radiation with a sphere of radius  $a$  are cross sections  $\sigma_i$  normalized to the geometrical particle cross section,  $\sigma_g = \pi a^2$  where  $ext$ ,  $abs$ ,  $sca$  and  $b$  stand for extinction, absorption, scattering and backscattering.

Energy conservation requires that [9]:

$$Q_{ext} = Q_{sca} + Q_{abs}, \text{ or } \sigma_{ext} = \sigma_{sca} + \sigma_{abs} \quad (6)$$

$$Q_{sca} = \frac{\sigma_{sca}}{\pi a^2} = \frac{2}{x^2} \sum_{n=1}^{\infty} (2n+1) (|a_n|^2 + |b_n|^2) \quad (7)$$

$$Q_{ext} = \frac{\sigma_{ext}}{\pi a^2} = \frac{2}{x^2} \sum_{n=1}^{\infty} (2n+1) \text{Re}(a_n + b_n) \quad (8)$$

The backscattering efficiency, applicable to monostatic radar, is given by Bohren and Huffman, [9]:

$$Q_b = \frac{\sigma_b}{\pi a^2} = \frac{1}{x^2} \left| \sum_{n=1}^{\infty} (2n+1) (-1)^n (a_n - b_n) \right|^2 \quad (9)$$

The index  $n$  runs from  $1$  to  $\infty$ , but the infinite series occurring in Mie formulas can be truncated at a maximum  $n_{\max}$ . For this number Bohren and Huffman [9, pg 470] proposed:

$$n_{\max} = x + 4x^{1/3} + 2 \quad (10)$$

and this value is used here. The size parameter is given by  $x = ka$ ,  $a$  is the radius of the sphere and  $k = 2\pi/\lambda$  is the wave number,  $\lambda$  the wavelength in the ambient medium, and

$$m = (\epsilon_1 \mu_1)^{1/2} / (\epsilon \mu)^{1/2} \quad (11)$$

is the refractive index with respect to the ambient medium.  $\epsilon_1$  and  $\mu_1$  are the permittivity and permeability of the sphere, and  $\epsilon$  and  $\mu$  are the permittivity and permeability of the ambient medium. Refraction index of water for wavelengths from  $10 \text{ nm}$  to  $10 \text{ m}$  as given in [10] where at  $f = 19.5 \text{ GHz}$  or  $15 \text{ mm}$  is  $6.70992 + 2.76083 i$ .

The backscattered far fields [11] in spherical coordinates  $(E_\theta, E_\phi)$  for a unit amplitude incident field is given by

$$E_\theta = [\exp(i\omega t - ikr) / ikr] S(\pi) \cos \phi, \quad (12)$$

$$E_\phi = [\exp(i\omega t - ikr) / ikr] S(\pi) \sin \phi, \quad (13)$$

Where

$$S(\pi) = \sum_{n=1}^{\infty} (-1)^n (n+1/2) (a_n - b_n). \quad (14)$$

The Mie scattering coefficients,  $a_n$  and  $b_n$ , are expressed in terms of the spherical Bessel functions, with  $a_n$  related to the amplitudes of the oscillations of magnetic type, while the coefficients  $b_n$  related to the amplitudes of electric oscillations, [11].

## II. RADAR EQUATIONS

Consider  $T_x$  as a transmitter illuminating a particle at a large distance  $r_1$  with a total power transmitted  $P_t$  and  $G_t(j_i)$  is the gain of transmitter in the incidence direction. Consider again  $R_x$  as a receiver of the scattered wave at a large distance  $r_2$  with the received power  $P_r$ . Assume that  $r_1$  and  $r_2$  are large and that the particle is in the far field of both antennas. The incident power flux density  $S_i$  at the particle in term of gain of transmitter, is given by

$$S_i = \frac{G_t(j_i)}{4\pi r_1^2} P_t \quad (15)$$

At the receiver, the power flux density  $S_r$  is given by

$$S_r = \frac{\sigma_{bi}(k_s, j_i)}{4\pi r_2^2} S_i \quad (16)$$

Where  $\sigma_{bi} = \sigma_{bi}(k_s, j_i)$  is the measure of the amount of incident power intercepted by the target and reradiated back in the direction of receiving radar, and is denoted as the radar bistatic cross section. Then the receiving power is given by

$$P_r = A_r(k_s) S_r \quad (17)$$

Where  $A_r(k_s)$  is the receiving cross section given by [4]

$$A_r(k_s) = \frac{\lambda^2}{4\pi} G_r(-k_s) \quad (18)$$

Equations (1) to (4) give a ratio of the received to the transmitted power

$$\frac{P_r}{P_t} = \frac{\lambda^2 G_t(j_i) G_r(-k_s) \sigma_{bi}(j_i, k_s)}{(4\pi)^3 r_1^2 r_2^2} \quad (19)$$

When  $k_s = -j_i$  and  $r_1 = r_2 = r$ , the ratio of the received to the transmitted power will be:

$$\frac{P_r}{P_t} = \frac{\lambda^2 (G_r(j_i))^2 \sigma_b(-j_i, j_i)}{(4\pi)^3 r^4} \quad (20)$$

The equation (19) is applied to bistatic radar while the equation (20) is for monostatic radar. For the rest of this paper we are going to concentrate on monostatic radar.

### III. THE FIRST ORDER MULTIPLE SCATTERING

The first order multiple scattering takes into account attenuation by scattering and absorption of a wave propagating along a path. This method is often used in millimeter and optical wave propagation through rain, fog, smog, and snow [4]. The first order multiple scattering can be easily considered as an extension of the radar equations for the single scattering approximation, discussed earlier in the preceding section.

The received power  $P_r$  given in (17) can be then modified for the first-order multiple scattering case as follows [8]:

$$P_r = \frac{\pi^5 P_t A_e h}{32 r^2 \lambda^4} \exp(-2\gamma r) \sum_i D^6 |K|^2 \quad (21)$$

where  $\gamma$  is the one-way attenuation coefficient, given by

$$\gamma = \int_0^r \rho < \sigma_{ext} > ds \quad (22)$$

The number of particles (or density)  $\rho(s_i)$  and the total cross section  $\sigma_{ext}(s_i)$  can be a function of the position along the path from the transmitter to  $dv$ . This can be easily incorporated in the (24) by substituting the total cross section  $\sigma_{ext}$  and the backscattered cross section  $\sigma_b$  with their average value defined in the following manner [4]

$$\rho < \sigma_{ext} > = \int_0^\infty n(D, r) \sigma_{ext} dD \quad (23)$$

$$\rho < \sigma_b > = \int_0^\infty n(D, r) \sigma_b dD \quad (24)$$

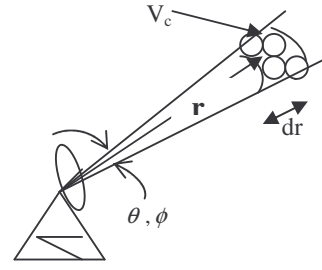


Fig. 2. Narrow beam monostatic radars.  $\theta$  and  $\phi$  are the half-power beamwidths in the vertical and horizontal directions, respectively [12]

The two-way attenuation of radar signal in traversing the distance  $r$  and back is an exponential function of the distance is given by

$$\psi = \exp(-2 \int_0^r \gamma dr) \quad (25)$$

For the backscattering radar equation (24), we obtain the rain cell volume,  $V_c$ , (Fig. 2):

$$V_c = (\pi r^2 \theta \phi / 4 \ln 2) dr \quad (26)$$

We then write (20) as:

$$\frac{P_r}{P_t} = (2.855 \times 10^{-4}) \lambda^2 [G_t(i_0)]^2 \theta \phi \int_{r_0}^r \frac{\rho \sigma_b}{r^2} e^{-2\gamma} dr \quad (27)$$

where  $(2.855 \times 10^{-4}) = \pi / (4\pi)^3 (8 \ln 2)$ .

The gains  $G_t(j_i)$  and  $G_r(k_s)$  are related to the actual aperture areas  $A_t$  and  $A_r$  of the transmitter and receiver:

$$G_t(j_i) = \eta_t 4\pi A_t / \lambda^2, \quad G_r(k_s) = \eta_r 4\pi A_r / \lambda^2 \quad (28)$$

Where  $\eta_t$  and  $\eta_r$  are the aperture efficiencies of the transmitter and the receiver, and are typically 0.5-0.6. The half-power beamwidths,  $\theta$  and  $\phi$  are related to the diameters of the apertures.  $\theta$  is given in terms of the diameter  $D_1$  in the  $\theta$  plane:

$$\theta = \alpha_1 \lambda / D_1 \quad \text{radians} \quad (29)$$

The constant  $\alpha_1$  is typically 1.3-1.6, depending on the field distribution over the aperture. We may combine (28) and (29) and obtain the following formula for the gain:

$$G_t(j_i) = (\eta_t \alpha_1 \alpha_2) (\pi^2 / \theta \phi) \approx \pi^2 / \theta \phi \quad (30)$$

The total backscattering cross section  $\rho < \sigma_b >$  per cubic meter of rain cell volume  $V_c$  in the beam can be obviously equated from (30) as follows, [12]:

$$\rho < \sigma_b > = \frac{114}{\chi^2 [G_i(j_i)]^2 \theta \phi e^{(-2\rho < \sigma_i > r)} \int_r^{r+dr} \frac{e^{(-2\rho < \sigma_i > r)}}{r^2} dr} \left( \frac{P_r}{P_t} \right) \quad (31)$$

So far, the attenuating effect of the precipitation  $e^{-2\gamma}$ , through which the signal may have to pass, has been considered. It shows that the influence of the rain intensity over the attenuation makes it difficult to determine the backscattering cross section  $\rho < \sigma_b >$  of the rain using (31) by only measuring the received power. Most of parameters in (31) are either known or measured. At frequencies higher than 10 GHz, the calculations of the cross sections must be made by using the Mie theory. The specific backscattering  $\gamma_b$  is given by [13]

$$\gamma_b = 0.25\pi \int_0^\infty D^2 Q_b N(D) dD \quad (32)$$

To convert the backscattering coefficient to dB/km we have to multiply with a factor of 4.343 and  $\gamma$ , attenuation coefficient in dB, can be found in [6-7] where it is characterized by path attenuation due rain in Durban between two campuses.

In absence of precipitation (dry weather), the received signal-to-noise ratio is given by, [14]:

$$\left( \frac{S}{N} \right)_d = \frac{P_d}{N_r} = \frac{K_1 \sigma_r / r_d^4}{N_r} \quad (33)$$

Where  $P_d$  = received echo power from a target of cross section  $\sigma_r$  at a range  $r_d$  in dry air;

$K_1$  = a constant representing the parameters of radar equation  
 $K_1 = P_t G^2 \chi^2 / (4\pi)^3$

$N_r$  = receiver noise power.

In inclement weather the signal-to-noise ratio is,

$$\left( \frac{S}{N} \right)_w = \frac{P_w}{N_r + P_r} = \frac{K_1 \sigma_r \psi / r_w^4}{N_r + P_r} \quad (34)$$

Where  $P_w$  = received echo power from a target of cross section  $\sigma_r$  at a range  $r_w$  in inclement weather.

$P_r$  = received echo power from rain is equal to equation (21).

$\psi = \exp(-2\gamma r_w)$  and  $\gamma$  = attenuation coefficient

When received echo power from rain becomes significant, it contributes to rise in the noise floor and the radar can lose the target.

#### IV. SPECIFIC RAIN BACKSCATTERING FOR DURBAN

Based on measurement realized by Naicker [6], we establish the specific rain backscattering (dB/km) using equation (32) for the Marshall-Palmer (MP), Joss-Drizzle (JD), Joss-Thunderstorm (JT) and Law-Parson (LP) distribution as exponential distribution; Continental-Showers (CS), Tropical Showers (TS), Continental Thunderstorms (CT) and Tropical Thunderstorm (TT) distribution as lognormal distribution at 19.5 GHz as show in Fig. 4. For TS, the minimum is occurs at rain rate equals of 1 mm/h and it maximum is at 5 mm/h with 7dB/km. We

see that from 10 mm/h to 79 mm/h, TS decreases slightly with approximate difference equal to 0.5dB/km. For CS, the minimum is 3dB/km with 1 mm/h, while the maximum of 4.3dB/km occurs at rain rate of 5 mm/h. For 20 mm/h to 79 mm/h the variation of the specific is approximately equals to 0.9dB/km. For TT, the minimum occurs at rain rate of 1 mm/h and to it peaks at 3 mm/h with 2.5dB/km. We see that from 10 mm/h to 79 mm/h, TT decreases and reaches 1.2dB/km.

For MP, JT, JD and LP, we observe that the specific backscattering increases more strongly with rain rate up to 10 mm/h and after that the increment is not significant while the rain rate is increasing; the maximum are 5dB/km, 4 dB/km, 2.5 dB/km and 5 dB/km, respectively. Also according to Laws and Parsons [15], a very big fraction of raindrops are larger than  $D \geq 1mm$  at rainfall intensities  $R \geq 2.5 mm/h$ . Therefore based on the scattering matrix by Bohren and Huffman, [9, pp 111], the angular diagrams for Mie scattering on raindrops at  $f = 19.5GHz$ ,  $T = 293^{\circ}K$  in Durban will appear as shown in Fig. 3. Mie scattering intensities as a function of  $\cos \theta$ , the upper part of the curves ( $0 < \theta < \pi$ ) are for polarization perpendicular to the scattering plan, and the lower part of the curves ( $\pi < \theta < 2\pi$ ) are for polarization parallel to the scattering plane and both functions are symmetric with respect to both half circles. The Mie backscattering efficiency on raindrop  $Q_b$  in figure 5 shows different maxima according to raindrop diameter. While the monostatic radar signal from rain is not directly influenced by the changing diagram, the modeling of microwave transmission signals depends on the angular diagram, i.e. on the phase function [4].

#### V. CONCLUSION

For rainfall intensity below about 10 mm/h for JD, JT, MP and LP distributions, and below about 4 mm/h for TS, TT, CT and CS distributions, the rain drops are small with respect to the wavelength at 19.5 GHz; the specific backscattering follows Rayleigh scattering law where the average backscattering cross section is proportional to the sixth power of the drop diameter [4, Chap. 3]. This can be seen in the curve observed in Fig. 4. For rainfall intensity above about 10 mm/h, the diameters of raindrops are in the order of the wavelength, so backscattering is predominantly due to Mie scattering law where the average backscattering cross section depends weakly on raindrop diameter. Since the raindrop diameter  $D$  appears as the sixth power in equation (21), it follows that in any raindrop size distribution, the small number of large drops will contribute the largest amount of received echo power of the rain. Then there is a reduction of the signal-to-noise ratio and the radar can lose the target according to equation (34). Fig. 5 shows that the highest Mie backscattering on raindrops in Durban at  $f = 19.5GHz$  occurs when  $D$  equals 4.7mm, and the lowest when  $D$  equals 1mm.

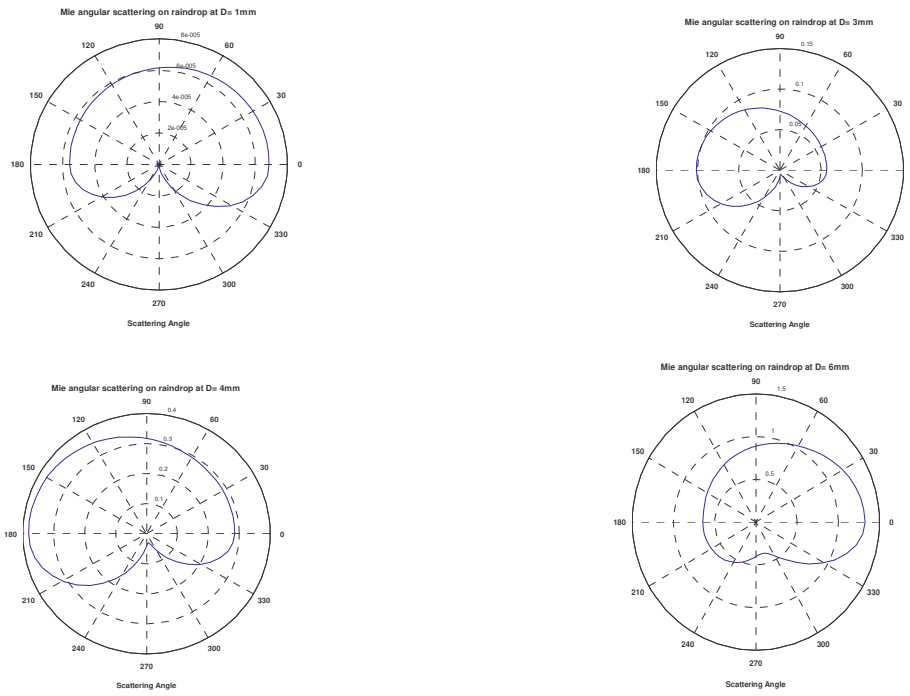


Fig. 3. Angular diagrams for Mie scattering on raindrops at  $f = 19.5\text{GHz}$  and  $T = 293\text{K}$  for different diameters ( $D=1,3,4$  and  $6\text{mm}$ )

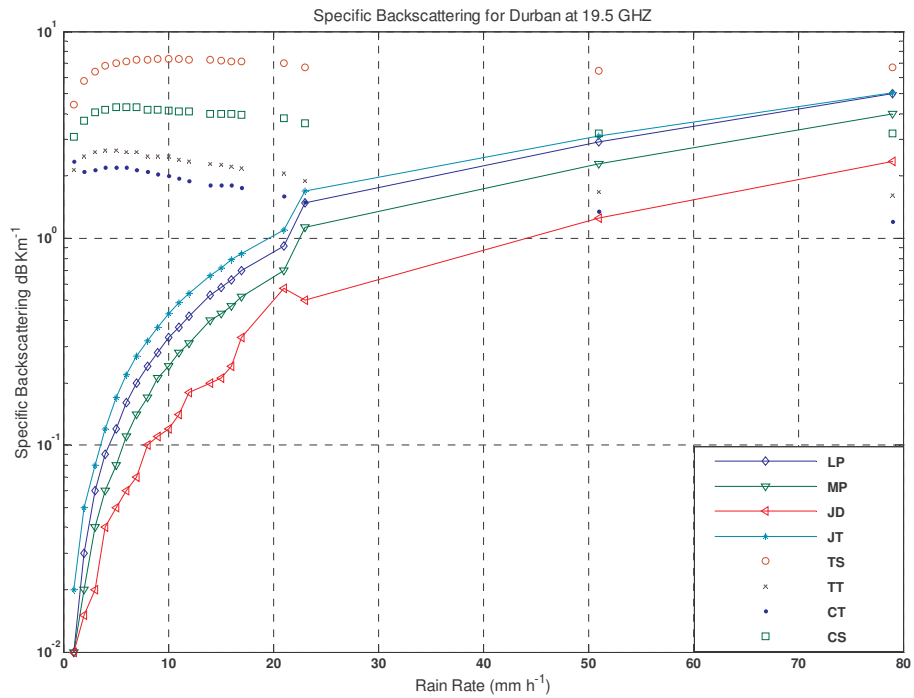


Fig. 4. Specific Rain backscattering in Durban for different distributions

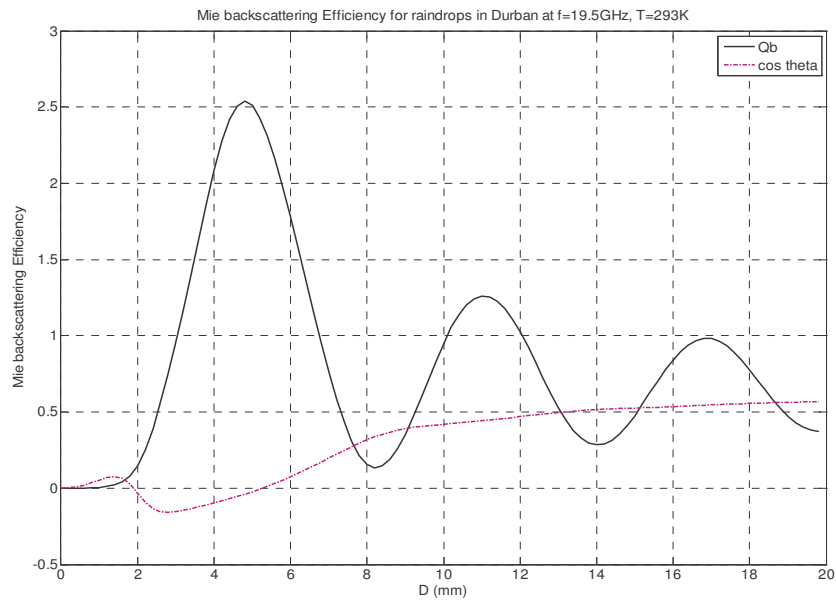


Fig. 5. Mie efficiencies on raindrop in Durban at  $f = 19.5\text{GHz}$  and  $T = 293\text{ }^{\circ}\text{K}$

#### REFERENCES

- [1] Joseph Nemarich, Ronald J. Wellman and James Lacombe, "Backscatter and attenuation by falling snow and rain at 96, 140, and 225 GHz," *IEEE Trans. Geoscience and Remote Sensing*, 26:319-329, May 1988.
- [2] Takeshi Manabe, Toshio Ihara, and Jun Awaka, "The relationship of raindrop-size distribution to attenuations experienced at 50, 80, 140 and 240 GHz," *IEEE Trans. on Antennas and Propagation*, AP-35:1093-1096, November 1987.
- [3] M. M. Z. Kharadly, "Scattering by rain and melting snow," *IEEE Trans. Antenna and Propagation*, 2:406-410, 1989.
- [4] Akira Ishimaru *Wave Propagation and Scattering in Random Media*, volume 1 and 2. Academic Press, New York, 1978.
- [5] Jonathan H. Jiang and Dong L. Wu, "Ice and water permittivity for millimeter and sub-millimeter remote sensing applications," *Atmospheric Science Letters*, March 31, 5:146-151, 2004.
- [6] K. Naicker and S. H. Mneney, "Propagation of measurements and multipath channel modeling for line-of-sight links at 19.5 GHz", *SAIEE Res. J.*, 97(2), 162-171, 2006.
- [7] M.O. Fashuyi and T.J. Afullo, Rain attenuation prediction and modeling for line-of-sight links on terrestrial paths in South Africa, *Radio Sci.*, 42, RS5006, doi:10.1029/2007RS003618.
- [8] M. I. Skolnik. *Radar Systems*, 2nd Edition McGraw-Hill, Inc., New York, 1962.
- [9] C.F. Bohren and D.R. Huffman, *Absorption and Scattering of Light by Small Particles*, John Wiley: New York, NY, 1983.
- [10] D. J. Segelstein: The complex refractive index of water, in physics, *University of Missouri*, Kansas City, 1981.
- [11] Hitoshi Inada, "New Calculation of Surface Wave Contributions Associated with Mie Backscattering," *Applied Optics*, Vol. 12, No. 7, July 1973
- [12] Alebel Arage Hassen, "Indicators for the Signal Degradation and Optimization of Automotive Radar Sensors under Adverse Weather Conditions," PhD Dissertation, *Technischen Universität Darmstadt*, Darmstadt 2006.
- [13] C. Mätzler, "Effects of rain on propagation, absorption and scattering of microwave radiation based on the dielectric model of Liebe," *IAP Res. Rep. No. 02-10*, University of Bern, June, 2002.
- [14] S. Silver, "Microwave Antenna Theory and Design," McGraw-Hill, New York, 1949.
- [15] J. Alfred, Jr. Bogush, "Radar and the Atmosphere," Artech House, Inc., MA, 1989.

**Chrispin T. Mulangu** holds B. Eng. Electronic Engineering (Kinshasa-D.R.Congo). He is currently pursuing his MSc. Eng. in Electronic Engineering at University of KwaZulu-Natal and he received Young Scientist Award XXIXth General Assembly URSI/Chicago-USA 2008.

**Thomas J. Afullo** holds PhD in Electrical Engineering from the Vrije Universiteit Brussel (VUB), Belgium. He is currently Associate professor, Dept. Electrical Engineering, University of KwaZulu-Natal (UKZN), Durban, South Africa.